Research Article

Stable Hybrid Fuzzy Controller-based Architecture for Robotic Telesurgery Systems

Radu-Emil Precup[1*], Tamás Haidegger[2], and Levente Kovács[2]

Abstract

Robotic surgery and remotely controlled teleoperational systems are on the rise. However, serious limitations arise on both the hardware and software side when traditional modeling and control approaches are taken. These limitations include the incomplete modeling of robot dynamics, tool–tissue interaction, human–machine interfaces and the communication channel. Furthermore, the inherent latency of long-distance signal transmission may endanger the stability of a robot controller. All of these factors contribute to the very limited deployment of real robotic telesurgery. This paper describes a stable hybrid fuzzy controller-based architecture that is capable of handling the basic challenges. The aim is to establish high fidelity telepresence systems for medical applications by easily handled modern control solution.

Keywords: Linear Matrix Inequality; Master–slave surgical robot architecture; Remote robot; Stable controller design; Takagi–Sugeno–Kang PI–fuzzy controller

1. Introduction

Remote monitoring, diagnostics and even telementoring have become regular tools of modern medicine. Nevertheless, due to the nature and complexity of surgery, remote systems are still limited to some notable examples, such as the da Vinci Surgical System (Fig. 1) from Intuitive Surgical Inc. (Sunnyvale, CA). The da Vinci system does not allow larger separation between the master and the slave side, thus alternative systems and control methods have to be developed for real (medium/long distance) telesurgery.

Long-distance surgical procedures supported, or performed by robots would open up new frontiers in medical interventions. This was the initial idea behind the first concepts when they appeared at NASA in the early 1970s (Haidegger, 2012). While the concept of telesurgery in space never lived beyond simulations, by 2001, it was possible for the first time to perform surgery on the basis of

_____

*Corresponding e-mail: radu.precup@upt.ro

1* Department of Automation and Applied Informatics, Politehnica University of Timisoara, Bd. V. Parvan 2, 300223 Timisoara, Romania

2 Antal Bejczy Center for Intelligent Robotics, Óbuda University, Kiscelli utca 82, 1032 Budapest, Hungary

ISDN-based intercontinental communication (Haidegger et al., 2011b). This proved that in urgent cases—in theory—doctors could reach out to patients hundreds or thousands of kilometers away. The interventions could be executed in places difficult to reach (remote rural areas) or dangerous for people (war zone). DARPA (the advanced research branch of the U.S. Department of Defense) has sponsored various projects—most notably the TRAUMA POD—to develop a technology that supports injured soldiers on the battlefield without risking the Medical Doctors' life (Garcia et al., 2009). Nevertheless, the difference in the complexity between supporting a distant operation on Earth and one in space is huge. Human space exploration is unimaginable without full medical support, yet it is impossible to send an entire medical crew with the spacecraft because of the high costs and the limited space. Some weird alternative concepts also emerged, e.g., a Dutch consortium announced plans to recruit for a one-way Mars mission (Mars One, 2013). The severe constraint of space and launch-weight keeps the research open towards telesurgical solutions, since many of the possibly emerging problems could be solved with one surgical robot sent along the expedition. Thus, proper modeling and control of both master and slave side remains an important research topic (Haidegger et al., 2011b). Communication with the surgical crew on Earth creates further tasks to solve. Most of the problems are caused by signal latency, which get worse with the increase of the range of the mission. Some of the disturbing effects of a generally proposed teleoperational surgical robotic system can be reduced by well-chosen system architecture and control. Currently feasible options are investigated in this paper.

Fig. 1. The fourth generation da Vinci Surgical System, the Xi, introduced in 2014. (Courtesy of Intuitive Surgical Inc.).

Just as in the case of other teleoperational systems, surgical robots also have three major components from the modeling and control point of view: master device, slave device and the communication system (Jordan et al., 2013). On the top of that, the tool–tissue interaction should also be assessed (Takacs et al., 2014), as long as there is physical interaction between the robotic tool and the patient. The modeling of these components is indispensable in order to build a valid simulator for the whole system to observe and analyze certain control attributes and behaviors.

The master side is where the "human operator" or the replacing automatic control device is located. Further, the surgical staff can be found here, providing the control signals for the actuators of the

slave. A commonly used human model is the crossover model that was developed in the 1960s for fighter pilots (Kleinman et al., 1970). It is based on the highly non-linear and time-dependent response of the human body, but it is well-approximated by a quasi-linear model.

The effect of time delay could be reduced with latency-tolerant control methods, thus larger distances can be bridged by these systems (Haidegger et al., 2012). To achieve this, robust models of the system components are required. The complete architecture is proposed to be approximated with three models. The master includes the controller and the human operator, which is connected via a high-delay medium to the slave model that covers the intervening master arm. In the deriving cascade setup, the time delay can be partially alleviated using appropriate predictive controllers tuned to the master and slave systems (Precup et al., 2012a).

While not all of the latencies can be avoided, empowering the slave system with autonomous capabilities can also improve functionality and safety. Robust control methods may further reduce the effect of latency. The slave robot's kinematic model is typically given to a fine level of details, enabling its integration into kinematic and dynamic models (Sun et al., 2007; Syed et al., 2012).

This paper is built upon our previous results in the fuzzy control of master–slave telesurgery applications (Haidegger et al., 2010; Haidegger et al., 2011a; Haidegger et al., 2012; Precup et al., 2011c; Precup et al., 2012a) and on our previous results on cost effective design and implementation of fuzzy controllers (Precup and Preitl, 1997; Precup and Preitl, 1999; Precup and Preitl, 2006a; Precup et al., 2004; Precup et al., 2011a; Preitl and Precup, 1997; Preitl et al., 2006), and it proposes a cascade control architecture to deal with the control of a remote robot performing surgical actions. A Takagi–Sugeno–Kang PID–fuzzy controller is suggested and implemented as an outer loop controller in the framework of a master–slave control system architecture dedicated to telesurgical robotic applications. The design of the Takagi–Sugeno–Kang PID–fuzzy controller is supported by the Linear Matrix Inequality (LMI)-based stability analysis of the fuzzy control system. Therefore, the stable design of the Takagi–Sugeno–Kang PID–fuzzy controller is carried out.

2. Fuzzy Control System Architecture and Stable Design

The cascade Control System Architecture (CSA) is applied in order to ensure good control system performance indices in the framework of the master–slave surgical robot architecture (Haidegger et al., 2011a; Haidegger et al., 2012; Precup et al. 2011c). The inner control loop represents the slave loop or the robot part of this CSA, while the outer control loop means the master loop or the human part of the CSA. The transfer functions specific to the CSA of the inner loop will be first presented in terms of the blocks of the cascade CSA illustrated in Fig. 2, which corresponds to the linear control case.

The simplified model of the slave robot is:

$$W_S(s) = \frac{(k_S + B_S s)G(s)}{s[M_S s^2 + B_S s + k_S + G(s)]}, \quad G(s) = k_t, \tag{1}$$

where k_S, B_S and M_S are the parameters of a reasonably small slave robot that can fit the long duration space missions, $G(s)$ is the tissue interaction model (Haidegger et al., 2010), and k_t is the tissue interaction gain. The tissue filter:

$$W_{F\_in}(s) = \frac{k_S}{B_S s + k_S} \qquad (2)$$

is applied to compensate the nominator of $W_S(s)$. Equations (1) and (2) lead to the transfer function of the process in the inner control loop:

$$W_P(s) = W_{F\_in}(s) W_S(s) = \frac{k_t k_S}{s(M_S s^2 + B_S s + k_t + k_S)} = \frac{k_P}{s(1 + T_1 s)(1 + T_\Sigma s)}, \qquad (3)$$

where k_P is the process gain of the inner control loop, T_1 is the large time constant and T_Σ is the small time constant with the expressions:

$$k_P = \frac{k_t k_S}{k_t + k_S}, \quad T_1 = \frac{2M_S}{B_S - \sqrt{B_S^2 - 4M_S(k_t + k_S)}}, \quad T_\Sigma = \frac{2M_S}{B_S + \sqrt{B_S^2 - 4M_S(k_t + k_S)}}. \qquad (4)$$
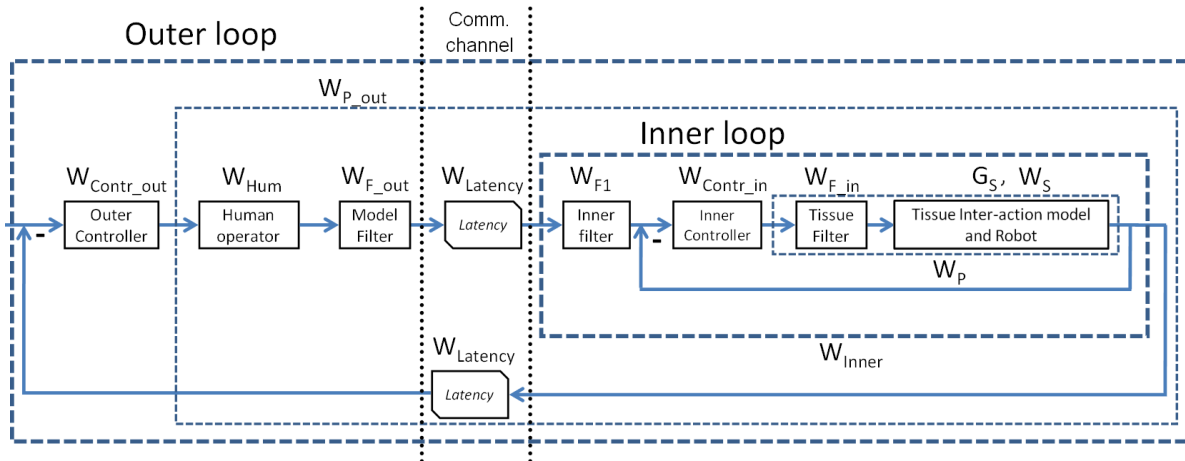

Fig. 2. Cascade CSA for telesurgery (Haidegger et al., 2011a)

Applying the Extended Symmetrical Optimum (ESO) method (Preitl and Precup, 1996; Preitl and Precup, 1999), the following inner PID controller transfer function results (Haidegger et al., 2011a):

$$W_{Contr\_in}(s) = \frac{k_{Contr\_in}}{s} (1 + T_{C1}s)(1 + T_{C2}s), \qquad (5)$$

with the tuning equations:

$$k_{Contr\_in} = \frac{1}{\beta\sqrt{\beta}k_P T_\Sigma^2}, \quad T_{C1} = T_1, \quad T_{C2} = \beta T_\Sigma, \tag{6}$$

where $\beta = \beta_{Inner}$, $4 \le \beta_{Inner} \le 20$, is the tuning parameter of the inner control loop.

For $4 \le \beta_{Inner} \le 9$, due to the complex conjugate poles in the closed-loop transfer function $W_C(s)$ given in (Preitl and Precup, 1996; Preitl and Precup, 1999), the inner filter with the transfer function $W_{F1}(s)$ is applied:

$$W_{F1}(s) = \frac{1 + (\beta - \sqrt{\beta})T_\Sigma s + T_\Sigma^2 s^2}{(1 + \beta T_\Sigma s)[1 + (\beta - \sqrt{\beta})T_\Sigma s]}, \tag{7}$$

and the closed-loop transfer function of the inner control loop is:

$$W_{Inner}(s) = W_{F1}(s)W_C(s) = \frac{1}{(1 + T_{P1}s)(1 + T_{P2}s)}, \quad T_{P1} = \sqrt{\beta}T_\Sigma, \quad T_{P2} = (\beta - \sqrt{\beta} - 1)T_\Sigma. \tag{8}$$

For the design of the outer loop, the human operator's model is characterized by the following transfer function (Haidegger et al., 2011a):

$$W_{Hum}(s) = k_{p\_Hum} \frac{\omega_{c\_Hum}}{s} e^{-sT_{Hum}}, \tag{9}$$

where k_{p_Hum} is the human operator gain, ω_{c_Hum} is the crossover frequency indicating the limitation of the human operator's reaction based on the information feedback, and T_{Hum} is the human operator's physiological latency. The outer loop filter (Haidegger, 2011)

$$W_{F\_out}(s) = \frac{1 + sT_{Comp}}{1 + sT_F} \tag{10}$$

is introduced to speed up the system, where T_{Comp} is set to compensate for the largest time constant of $W_{Inner}(s)$:

$$T_{Comp} = \max(T_{P1}, T_{P2}), \tag{11}$$

and T_F is a small filtering time constant that fulfils the condition (Haidegger, 2011):

$$0 < T_F << \min(T_{P1}, T_{P2}) = T_{P3}. \tag{12}$$

Consequently, the transfer function of the process of the outer control loop results as (Haidegger et al., 2011a):

$$W_{P\_out}(s) = W_{Hum}(s)W_{F\_out}(s)W_{Latency}(s)W_{Inner}(s)W_{Latency}(s) = \frac{k_{P\_out}}{s(1+T_F s)(1+T_{P3} s)} e^{-sT_m}, \tag{13}$$

where k_{P_out} is the outer loop process gain and T_m is the outer loop process time delay:

$$k_{P\_Out} = k_{p\_Hum}\omega_{c\_Hum}, \quad T_m = T_{Hum}2T_d, \tag{14}$$

with T_d (the round-trip latency) corresponding to the two latency blocks shown in Fig. 2.

As shown in (Haidegger et al., 2011; Precup et al., 2011c), an outer loop PID controller with the transfer function:

$$W_{Contr\_out}(s) = \frac{k_{Contr\_out}}{s}(1+T_{C1out}s)(1+T_{C2out}s), \tag{15}$$

can be designed using a first order approximation of the time delay in (13) by means of the following tuning equations specific to the ESO method:

$$k_{Contr\_out} = \frac{1}{\beta\sqrt{\beta}k_{P\_out}(T_F + T_{P3})^2}, \quad T_{C1out} = T_m, \quad T_{C2out} = \beta(T_F + T_{P3}), \tag{16}$$

where $\beta = \beta_{Outer}$, $4 \le \beta_{Outer} \le 20$ is the tuning parameter of the outer control loop. As shown by Precup et al. (2011c), the outer loop PID controller with the transfer function (15) can be decomposed in a series connection of proportional–integral (PI) and proportional–derivative (PD) blocks with the transfer functions $W_{PI}(s)$ and $W_{PD}(s)$, respectively:

$$W_{Contr\_out}(s) = W_{PI}(s)W_{PD}(s), \quad W_{PI}(s) = \frac{k_{Contr\_out}}{s}(1+T_{C1out}s) = k_C\left(1+\frac{1}{T_i s}\right), \quad W_{PD}(s) = 1+T_{C2out}s, \tag{17}$$

where k_C is the gain of the PI controller and T_i is the integral time constant of the PI controller:

$$k_C = k_{Contr\_out}T_{C1out} = \frac{T_m}{\beta\sqrt{\beta}k_{P\_out}(T_F + T_{P3})^2}, \quad T_i = T_{C1out} = T_m. \tag{18}$$

However, the linear PI controller defined in (17) will be replaced by the Takagi–Sugeno–Kang PI–fuzzy controller in order to obtain the control system performance enhancement. Other fuzzy controller approaches can be used as well (Deliparaschos et al., 2006; Feriyonika and Dewantoro, 2013; Joelianto et al., 2013; Khanesar et al., 2011; Linda and Manic, 2011; Melin et al., 2013; Tikk et al., 2011). The continuous-time treatment of the Takagi–Sugeno–Kang PI–fuzzy controller will be presented as follows as a theoretically

justified counterpart of the discrete-time solutions discussed in the literature (Haidegger et al. 2011a; Haidegger et al., 2012; Precup et al. 2011c).

The membership functions of the Takagi–Sugeno–Kang PI–fuzzy controller are presented in Fig. 3, where $e(t)$ is the control error:

$$e(t) = r(t) - y(t), \tag{19}$$

$r(t)$ is the reference input (the robot position setpoint), $y(t)$ is the controlled output (the measured robot position), and $e_I(t)$ is the integral of control error and also the state variable of the integral part of the linear PI controller:

$$e_I(t) = \int_0^t e(\tau)d\tau. \tag{20}$$

The rule base of the Takagi–Sugeno–Kang PI–fuzzy controller is designed by introducing nine separately designed PI controllers and a fixed PD controller given in (17), with the parameters k_C^k and T_i^k of the PI controllers placed in the rule consequents, where $k = 1...9$ is the index of the current rule in a complete rule base. The linear PI controllers are tuned using the ESO-based tuning equations (18). Therefore the Takagi–Sugeno–Kang PI–fuzzy controller exhibits the behavior of a bumpless interpolator between several separately tuned linear PI controllers with the transfer functions $W_{PI}(s)$. Different values of the design parameter $\beta = \beta_{Outer}$ referred to as β^k, $k = 1...9$, are used in this context, in order to exploit and combine the advantageous performance of the cascade CSA with linear PI controllers in the outer control loop.
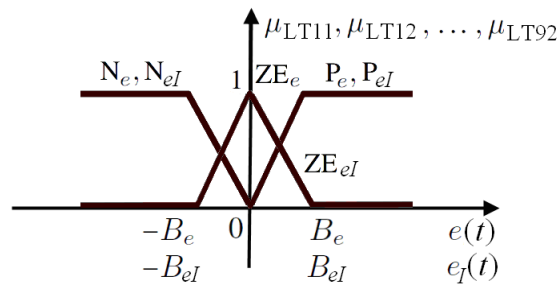

Fig. 3. Input membership functions of Takagi–Sugeno–Kang PI–fuzzy controller.

The rule base of the Takagi–Sugeno–Kang PI–fuzzy controller is expressed as:

$$\text{Rule } 1: \text{IF } e(t) \text{ IS } LT_{11} = N_e \text{ AND } e_I(t) \text{ IS } LT_{12} = P_{eI} \text{ THEN } u^1(t) = k_C^1 e(t) + (k_C^1 / T_i^1) e_I(t),$$

$$\text{Rule } 2: \text{IF } e(t) \text{ IS } LT_{21} = ZE_e \text{ AND } e_I(t) \text{ IS } LT_{22} = P_{eI} \text{ THEN } u^2(t) = k_C^2 e(t) + (k_C^2 / T_i^2) e_I(t),$$

$$\text{Rule } 3: \text{IF } e(t) \text{ IS } LT_{31} = P_e \text{ AND } e_I(t) \text{ IS } LT_{32} = P_{eI} \text{ THEN } u^3(t) = k_C^3 e(t) + (k_C^3 / T_i^3) e_I(t),$$

$$\text{Rule } 4: \text{IF } e(t) \text{ IS } LT_{41} = N_e \text{ AND } e_I(t) \text{ IS } LT_{42} = ZE_{eI} \text{ THEN } u^4(t) = k_C^4 e(t) + (k_C^4 / T_i^4) e_I(t),$$

$$\text{Rule } 5: \text{IF } e(t) \text{ IS } LT_{51} = ZE_e \text{ AND } e_I(t) \text{ IS } LT_{52} = ZE_{eI} \text{ THEN } u^5(t) = k_C^5 e(t) + (k_C^5 / T_i^5) e_I(t),$$

$$\text{Rule } 6: \text{IF } e(t) \text{ IS } LT_{61} = P_e \text{ AND } e_I(t) \text{ IS } LT_{62} = ZE_{eI} \text{ THEN } u^6(t) = k_C^6 e(t) + (k_C^6 / T_i^6) e_I(t),$$

$$\text{Rule } 7: \text{IF } e(t) \text{ IS } LT_{71} = N_e \text{ AND } e_I(t) \text{ IS } LT_{72} = N_{eI} \text{ THEN } u^4(t) = k_C^4 e(t) + (k_C^4 / T_i^4) e_I(t),$$

$$\text{Rule } 8: \text{IF } e(t) \text{ IS } LT_{81} = ZE_e \text{ AND } e_I(t) \text{ IS } LT_{82} = N_{eI} \text{ THEN } u^5(t) = k_C^5 e(t) + (k_C^5 / T_i^5) e_I(t),$$

$$\text{Rule } 9: \text{IF } e(t) \text{ IS } LT_{91} = P_e \text{ AND } e_I(t) \text{ IS } LT_{92} = N_{eI} \text{ THEN } u^6(t) = k_C^6 e(t) + (k_C^6 / T_i^6) e_I(t),$$

$$(21)$$

where $u^k(t)$ is the control signal produced by k^{th} rule, $k = 1 \ldots 9$. Using the PROD operator to model the AND function in the rule antecedent, each fuzzy rule generates a firing degree α_k, $0 \le \alpha_k \le 1$, according to

$$\alpha_k(t) = \mu_{LTk1}(e(t)) \mu_{LTk2}(e_I(t)), \ k = 1 \ldots 9, \tag{22}$$

where μ_{LTkl} are the membership functions of the linguistic terms LT_{kl}, $k = 1 \ldots 9$, $l = 1 \ldots 2$, pointed out in Fig. 3 and in (21).

The weighted average defuzzification method produces the output of the Takagi–Sugeno–Kang PI–fuzzy controller represented by the control signal $u(t)$:

$$u(t) = \frac{\sum_{k=1}^{9} \alpha_k(t) u^k(t)}{\sum_{k=1}^{9} \alpha_k(t)} = \sum_{k=1}^{9} h_k(t) u^k(t) = \sum_{k=1}^{9} h_k(t)[k_C^k e(t) + (k_C^k / T_i^k) e_I(t)], \ h_k(t) = \frac{\alpha_k(t)}{\sum_{k=1}^{9} \alpha_k(t)}, \tag{23}$$

where $h_k(t)$ is the normalized firing degree of kth rule, $k = 1 \ldots 9$.

The stable design of the Takagi–Sugeno–Kang PI–fuzzy controller uses the state-space representation of the process. With this regard, the companion form of the transfer function $W_{FP\_out}(s)$ of the filtered process transfer function controlled by the PI block is:

$$W_{FP\_out}(s) = W_{PD}(s) W_{P\_out}(s) = \frac{k_{P\_out}[1 + \beta(T_F + T_{P3}) s]}{s(1 + T_F s)(1 + T_{P3} s)} e^{-s T_m} \tag{24}$$

for the average (constant) value of $\beta = \beta_{Outer}$ is:

$$\dot{\mathbf{x}}(t) = \mathbf{A}\,\mathbf{x}(t) + \mathbf{B}\,u(t - T_m),$$
$$y(t) = \mathbf{C}\,\mathbf{x}(t),$$

(25)

where $\mathbf{x}(t) = [x_1(t) \quad x_2(t) \quad x_3(t)]^T$ is the state vector of the filtered process in the outer control loop, T stands for matrix transposition, $x_1(t)$, $x_2(t)$ and $x_3(t)$ are the state variables, and the matrices in (25) are:

$$\mathbf{A} = \begin{bmatrix} 0 & 1 & 0 \\ 0 & 0 & 1 \\ 0 & -1 & -T_F - T_{P3} \end{bmatrix}, \quad \mathbf{B} = [0 \quad 0 \quad 1]^T, \quad \mathbf{C} = [k_{P\_out} \quad k_{P\_out}\beta(T_F + T_{P3}) \quad 0]^T.$$

(26)

The computation of the derivative of both terms in (20) using (19) and (25) leads to the dynamics of the integral part of the linear PI controller:

$$\dot{e}_I(t) = r(t) - \mathbf{C}\,\mathbf{x}(t).$$

(27)

But the unified expression of kth rule in the rule base of the Takagi–Sugeno–Kang PI–fuzzy controller results from (21):

Rule k : IF $e(t)$ IS LT_{k1} AND $e_I(t)$ IS LT_{k2} THEN $u^k(t) = k_C^k e(t) + (k_C^k / T_i^k)e_I(t)$, $k = 1...9$.

(28)

Using (19) and the second equation in (25) in (23), the expression of the control signal $u(t)$ is:

$$u(t) = \sum_{k=1}^{9} h_k(t)[k_C^k e(t) + (k_C^k / T_i^k)e_I(t)] = -\sum_{k=1}^{9} h_k(t)k_C^k \mathbf{C}\,\mathbf{x}(t) + \sum_{k=1}^{9} h_k(t)(k_C^k / T_i^k)e_I(t) + \sum_{k=1}^{9} h_k(t)k_C^k r(t).$$

(29)

Since $\sum_{k=1}^{9} h_k(t) = 1$, the substitution of $u(t)$ from (29) in (25) according to (27) leads to the sate-space model of the fuzzy control system:

$$\dot{\mathbf{x}}(t) = \sum_{k=1}^{9} h_k(t)[\mathbf{A}\,\mathbf{x}(t) - k_C^k \mathbf{B}\,\mathbf{C}\,\mathbf{x}(t - T_m) + (k_C^k / T_i^k)\,\mathbf{B}\,e_I(t - T_m) + k_C^k \mathbf{B}\,r(t)],$$

$$\dot{e}_I(t) = \sum_{k=1}^{9} h_k(t)[-\mathbf{C}\,\mathbf{x}(t) + r(t)],$$

$$y(t) = \mathbf{C}\,\mathbf{x}(t).$$

(30)

The extended state vector of the fuzzy control system is next defined as the vector $\mathbf{v}(t)$ by inserting $e_I(t)$ in $\mathbf{x}(t)$:

$$\mathbf{v}(t) = [\mathbf{x}^T(t) \quad e_I(t)]^T.$$

(31)

Therefore, the expression of the state-space model of the fuzzy control system employed in the LMI-based stability analysis of fuzzy control system results as follows from (30) in terms of the notation (31):

$$\dot{\mathbf{v}}(t) = \sum_{k=1}^{9} h_k(t)[\mathbf{A}_0\,\mathbf{v}(t) + \mathbf{A}_{kd}\,\mathbf{v}(t - T_m) + \mathbf{B}_{kr}\,r(t)],$$

$$y(t) = \sum_{k=1}^{9} h_k(t)\,\mathbf{C}_0\,\mathbf{v}(t),$$

(32)

with the matrices:

$$\mathbf{A}_0 = \begin{bmatrix} \mathbf{A} & \mathbf{0} \\ -\mathbf{C} & 0 \end{bmatrix},\ \mathbf{A}_{kd} = \begin{bmatrix} -k_C^k\,\mathbf{B}\,\mathbf{C} & (k_C^k/T_i^k)\,\mathbf{B} \\ 0 & 0 \end{bmatrix},\ \mathbf{B}_{kr} = \begin{bmatrix} k_C^k\,\mathbf{B} \\ 1 \end{bmatrix},\ \mathbf{C}_0 = [\mathbf{C}\quad 0],\ k = 1...9.$$

(33)

However, other stability analysis approaches can be used as well. Some representative approaches are given in (Baranyi, 2004; Precup and Preitl, 2006b; Precup and Preitl, 2007; Precup et al., 2009; Precup et al., 2012b; Preitl et al., 2002; Škrjanc and Blažič, 2005; Tomescu et al., 2007).

The stable design of the Takagi–Sugeno–Kang PI–fuzzy controller is carried out on the basis of the globally asymptotically stability of the equilibrium point of the fuzzy control system. For $\mathbf{B}_{kr} = \mathbf{0}$, $k = 1...9$, in the model (32), with these matrices considered as a disturbance input, the stability is guaranteed if there exists the common (i.e., for all rules) matrices $\mathbf{P} > 0$ and $\mathbf{R} > 0$, $\det \mathbf{R} \neq 0$, such that the following sufficient LMIs are fulfilled:

$$\mathbf{P}\,\mathbf{A}_0 + (\mathbf{A}_0)^T\,\mathbf{P} + \mathbf{P}\,\mathbf{A}_{kd}\,\mathbf{R}^{-1}\,(\mathbf{A}_{kd})^T\,\mathbf{P} + \mathbf{R} < 0,\quad k = 1...9.$$

(34)

The nine LMIs given in (34) are derived from (Gu et al., 2001), and their solving is assisted by numerical algorithms. Equation (34) is used in setting the values of the parameters of input membership functions defined in Fig. 3.

3. Case Study and Simulation Results

The case study uses the values for the parameters of the process: k_S = 400, B_S = 20 Ns/m, M_S = 0.1 kg, k_t = 0.0984, k_{P_Hum} = 0.5, ω_{c_Hum} = 2 rad/s, T_{Hum} = 0.1 s and T_d = 1 s. The following parameters are involved in the fuzzy controller design (Haidegger, 2011; Precup et al., 2011c): k_P = 0.098, T_1 = 0.044 s and T_Σ = 0.006 s for the inner control loop and β = $β_{Inner}$ =20, the PID controller for the slave part results in the following parameters: k_{Contr_in} = 3580.055, T_{C1} = 0.044 s and T_{C2} = 0.013 s, while the filter time constant is T_F = 0.003 s; k_{P_out} = 1, T_m = 2.1 s and T_{P3} = 0.025 s for the master control loop. Setting the tuning parameter β = $β_{Outer}$ =16, the PID controller parameters for the master control loop become k_{Contr_out} = 20.332, T_{C1out} = 2.1 s and T_{C2out} = 0.444 s; the corrections of two of tuning parameters of $W_{Contr\_out}(s)$ in order to account for the presence of time delays leads to the values k_{Cont_out} = 0.041 and T_{C1_out} = 5.25 s. Two separately designed outer PI controllers are used, the first one corresponds to the rules 3 and 7 of the rule base defined in (21), and the second one

corresponds to the rest of the rules. The first linear PI controller is characterized by a smaller gain, obtained from $\beta = \beta_{Outer} = 16$, in order to reduce the overshoot as the rules 3 and 7 are characterized by the same sign of the fuzzy controller inputs. The second linear PI controller is designed using the ESO method for the parameter $\beta = \beta_{Outer} = 9$. The parameters of the consequents of the Takagi–Sugeno–Kang PI–fuzzy controller obtain the values:

$$k_C^1 = k_C^2 = k_C^4 = k_C^5 = k_C^6 = k_C^8 = k_C^9 = 0.0723, \quad k_C^3 = k_C^7 = 0.0305,$$
$$T_i^1 = T_i^2 = T_i^3 = T_i^4 = T_i^5 = T_i^6 = T_i^7 = T_i^8 = T_i^9 = 5.25\,\text{s}.$$

(35)

The parameters of the input membership functions are set, such that to fulfill the LMI-based stability conditions (34): $B_e = 0.3$ and $B_{el} = 40$. The behavior of the cascade linear control system with respect to the unit step modification of the reference input is presented as the system output shown in Fig. 4 for the comparison with the fuzzy control system.
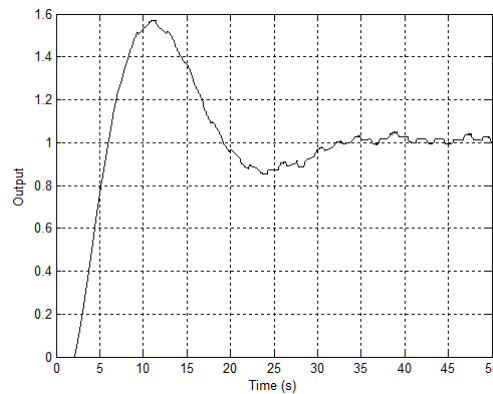

Fig. 4. Output (robot position) versus time for linear control system with outer PID controller.

The fuzzy control system was also tested by digital simulation with respect to the unit step modification of the reference input. The control system response is presented in Fig. 5, which proves that the proposed fuzzy controller ensures a small improvement of the control system performance indices expressed (overshoot and settling time).
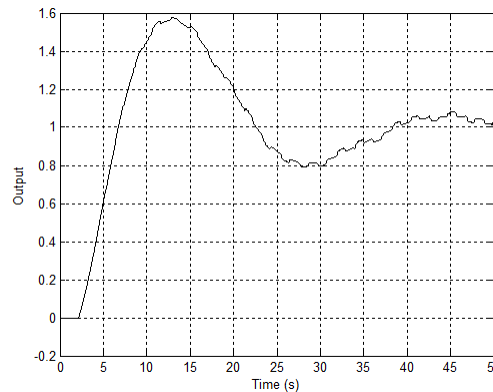

Fig. 5. Output (robot position) versus time for fuzzy control system with outer Takagi–Sugeno PI–fuzzy controller.

The performance offered by the Takagi–Sugeno–Kang PI–fuzzy controller is comparable to the performance of the control system with Takagi–Sugeno–Kang PID–fuzzy controller (Precup et al., 2012). The best performance is achieved by the Takagi–Sugeno–Kang PID–fuzzy controller, but the Takagi–Sugeno–Kang PI–fuzzy controller offers a better tradeoff to comparison and cost of implementation. Moreover, the single nonlinear element in the structure of Takagi–Sugeno–Kang PI–fuzzy controllers enables the simplified analysis and stable design.

The performance of the fuzzy control system can be further improved by the introduction of a setpoint filter for the outer control loop. However, the performance cannot be generalized to other applications (Bolla et al., 2014; Castillo et al., 2013; Dumitrache and Dragoicea, 2004; Horváth and Rudas, 2013; Lamár and Neszveda, 2013; Precup et al., 2011d; Shin et al., 2013; Škrjanc et al., 2004; Tang et al., 2014; Vaščák, 2010; Vaščák and Paľa, 2012), where several specific features should be accounted for and introduced in the fuzzy controller structure.

4. Conclusions

The realistic modeling of human tissue, tool–tissue interaction and a complex robotic device in a telesurgical setup is fundamental to realize high fidelity teleoperation control, especially when the quality of the network communication cannot be guaranteed in terms of QoS and latencies. The modeling performance can be improved by employed optimization techniques in the process modeling (Chan et al., 2013; David et al., 2013; Duran and Perez, 2013; Filip and Leiviskä, 2009; Formentin et al., 2012; Precup et al., 2011b).

The LMI-based stability conditions proposed in this paper are employed in the stable design of the fuzzy controller. The cost effective design and implementation is supported by a very simple controller structure. The case study shows good control system performance.

The control system performance must be improved as high fidelity telepresence systems for medical applications. The modification of controller structure can be used with this regard. Future research will be dedicated to the ACS performance improvement by systematic design using several controller structures with additional functionalities that include reduced sensitivity, high robustness to process parametric disturbances and uncertainties, and optimization regarding multiple performance indices.

Acknowledgements

References

Baranyi, P. (2004). TP model transformation as a way to LMI-based controller design. IEEE Transactions on Industrial Electronics, 51(2) 387–400.
http://dx.doi.org/10.1109/TIE.2003.822037

Bolla, K., Johanyák, Z. C., Kovács, T., & Fazekas, G. (2014). Local center of gravity based gathering algorithm for fat robots. In Issues and Challenges of Intelligent Systems and Computational Intelligence, L. T. Kóczy, C. R. Pozna, and J. Kacprzyk, Eds. Cham: Springer-Verlag, Studies in Computational Intelligence, vol. 530, pp. 175–183.

Castillo, L. F., Bedia, M. G., & Isaza, G. (2013). Exploration/exploitation in CBR systems: A formal analysis. International Journal of Artificial Intelligence, 11(A13) 46–56.

Chan, K. Y., Dillon, T. S., & Chang, E. (2013). An intelligent particle swarm optimization for short-term traffic flow forecasting using on-road sensor systems. IEEE Transactions on Industrial Electronics, 60(10) 4714–4725.
http://dx.doi.org/10.1109/TIE.2012.2213556

David, R.-C., Precup, R.-E., Petriu, E. M., Radac, M.-B., & Preitl, S. (2013). Gravitational search algorithm-based design of fuzzy control systems with a reduced parametric sensitivity. Information Sciences, 247 154–173.
http://dx.doi.org/10.1016/j.ins.2013.05.035

Deliparaschos, K. M., Nenedakis, F. I., & Tzafestas, S. G. (2006). Design and implementation of a fast digital fuzzy logic controller using FPGA technology. Journal of Intelligent and Robotic Systems, 45(1) 77–96.
http://dx.doi.org/10.1007/s10846-005-9016-2

Dumitrache, I., & Dragoicea, M. (2004). Intelligent techniques for cognitive mobile robots. Control Engineering and Applied Informatics, 6(2) 3–8.

Duran, O., & Perez, L. (2013). Solution of the spare parts joint replenishment problem with quantity discounts using a discrete particle swarm optimization technique. Studies in Informatics and Control, 22(4) 319–328.

Feriyonika, & Dewantoro, G. (2013). Fuzzy sliding mode control for enhancing injection velocity performance in injection molding machine. International Journal of Artificial Intelligence, 10(S13) 75–87.

Filip, F.-G., & Leiviskä, K. (2009). Large-scale complex systems. In Springer Handbook of Automation, S. Y. Nof, Ed. Berlin, Heidelberg: Springer-Verlag, pp. 619–638.
http://dx.doi.org/10.1007/978-3-540-78831-7_36

Formentin, S., Corno, M., Savaresi, S. M., & Del Re, L. (2012). Direct data-driven control of linear time-delay systems. Asian Journal of Control, 14(3) 652–663.
http://dx.doi.org/10.1002/asjc.387

Garcia, P., Rosen, J., Kapoor, C., Noakes, M., Elbert, G., Treat, M., Ganous, T., Hanson, M., Manak, J., Hasser, C., Rohler, D., & Satava, R. (2009). Trauma pod: A semi-automated telerobotic surgical system. International Journal of Medical Robotics and Computer Assisted Surgery, 5(2) 136–146.
http://dx.doi.org/10.1002/rcs.238

Gu, Y., Wang, H. O., Tanaka, K., & Bushnell, L. G. (2001). Fuzzy control of nonlinear time-delay systems: stability and design issues, In Proceedings of 2001 American Control Conference, Arlington, VA, USA, vol. 6, pp. 4771–4776.

Haidegger, T. (2011). Enhancing Computer-Integrated Surgical Systems – A Control Engineering Approach. Saarbrücken: LAP LAMBERT Academic Publishing.

Haidegger, T. (2012). Surgical robot prototyping – System development, assessment and clearance. In Prototyping of Robotic Systems: Applications of Design and Implementation, T. Sobh and X. Xiong, Eds. Bridgeport, CT: IGI Book, pp. 288–326.
http://dx.doi.org/10.4018/978-1-4666-0176-5.ch010

Haidegger, T., Kovács, L., Precup, R.-E., Benyó, B., Benyó, Z., & Preitl, S. (2012). Simulation and control for telerobots in space medicine. Acta Astronautica, 81(1) 390–402.
http://dx.doi.org/10.1016/j.actaastro.2012.06.010

Haidegger, T., Kovács, L., Preitl, S., Precup, R.-E., Benyó, B., & Benyó, Z. (2011a). Controller design solutions for long distance telesurgical applications. International Journal of Artificial Intelligence, 6(S11) 48–71.

Haidegger, T., Kovács, L., Preitl, S., Precup, R.-E., Kovács, A., Benyó, B., & Benyó, Z. (2010). Cascade control for telehealth applications. Scientific Bulletin of "Politehnica" University of Timisoara, Romania, Transactions on Automatic Control and Computer Science, 55(69)(4) 223–232.

Haidegger, T., Sándor, J., & Benyó, Z. (2011b). Surgery in space: the future of robotic telesurgery. Surgical Endoscopy, 25(3), 681–690.
http://dx.doi.org/10.1007/s00464-010-1243-3

Horváth, L., & Rudas, I. J. (2013). Active knowledge for the situation-driven control of product definition. Acta Polytechnica Hungarica, 10(2) 217–234.

Joelianto, E., Anura, D. C., Priyanto, M. P. (2013). ANFIS – hybrid reference control for improving transient response of controlled systems using PID controller. International Journal of Artificial Intelligence, 10(S13) 88–111.

Jordan, S., Takacs, A., Rudas I. J., & Haidegger, T. (2013). Modelling and control frameworfor robotic telesurgery. In Proceedings of 3rd Joint Workshop on New Technologies for Computer/Robot Assisted Surgery (CRAS 2013), Verona, Italy, pp. 89–92.

Khanesar, M. A., Kaynak, O., & Teshnehlab, M. (2011). Direct model reference Takagi-Sugeno fuzzy control of SISO nonlinear systems. IEEE Transactions on Fuzzy Systems, 19(5) 914–924.
http://dx.doi.org/10.1109/TFUZZ.2011.2150757

Kleinman, D. L., Baron, S., & Levison, W. H. (1970). An optimal control model of human response part I: Theory and validation. Automatica, 6(3) 357–369.
http://dx.doi.org/10.1016/0005-1098(70)90051-8

Lamár, K., & Neszveda, J. (2013). Average probability of failure of aperiodically operated devices. Acta Polytechnica Hungarica, 10(8) 153–167.

Linda, O., & Manic, M. (2011). Fuzzy Force-feedback augmentation for manual control of multirobot system. IEEE Transactions on Industrial Electronics, 58(8) 3213–3220.
http://dx.doi.org/10.1109/TIE.2010.2068532

Mars One (2013). Mars One press release: 78,000 sign up for one-way mission to Mars. http://mars-one.com, May 7, 2013.

Melin, P., Astudillo, L., Castillo, O., Valdez, F., & Garcia, M. (2013). Optimal design of type-2 and type-1 fuzzy tracking controllers for autonomous mobile robots under perturbed torques using a new chemical optimization paradigm. Expert Systems with Applications, 40(8) 3185–3195.
http://dx.doi.org/10.1016/j.eswa.2012.12.032

Precup, R.-E., David, R.-C., Petriu, E. M., Preitl, S., & Paul, A. S. (2011a). Gravitational search algorithm-based tuning of fuzzy control systems with a reduced parametric sensitivity. In Soft Computing in Industrial Applications, A. Gaspar-Cunha, R. Takahashi, G. Schaefer, and L. Costa, Eds. Berlin, Heidelberg: Springer–Verlag, Advances in Intelligent and Soft Computing, vol. 96, pp. 141–150.
http://dx.doi.org/10.1007/978-3-642-20505-7_12

Precup, R.-E., David, R.-C., Petriu, E. M., Preitl, S., & Radac, M.-B. (2011b). Gravitational search algorithms in fuzzy control systems tuning. In Proceedings of 18th IFAC World Congress, Milano, Italy, pp. 13624–13629.

Precup, R.-E., Haidegger, T., Kovács, L., Paul, A. S., Preitl, S., & Benyó, Z. (2012a). Fuzzy control solution for telesurgical applications. Applied and Computational Mathematics, 11(3) 378–397.

Precup, R.-E., Kovács, L., Haidegger, T., Preitl, S., Kovács, A., Benyó, B., Borbély, E., & Benyó, Z. (2011c). Time delay compensation by fuzzy control in the case of master-slave telesurgery. In Proceedings of 6th IEEE International Symposium of Computational Intelligence Informatics (SACI 2011), Timisoara, Romania, pp. 305–310.

Precup, R.-E., & Preitl, S. (1997). Popov-type stability analysis method for fuzzy control systems. In Proceedings of Fifth European Congress on Intelligent Technologies and Soft Computing (EUFIT'97), Aachen, Germany, vol. 2, pp. 1306–1310.

Precup, R.-E., & Preitl, S. (1999). Fuzzy Controllers. Timisoara: Editura Orizonturi Universitare.

Precup, R.-E., & Preitl, S. (2006a). Stability and sensitivity analysis of fuzzy control systems. Mechatronics applications. Acta Polytechnica Hungarica, 3(1) 61–76.

Precup, R.-E., & Preitl, S. (2006b). PI and PID controllers tuning for integral-type servo systems to ensure robust stability and controller robustness. Electrical Engineering, 88(2) 149–156.
http://dx.doi.org/10.1007/s00202-004-0269-8

Precup, R.-E., & Preitl, S. (2007). PI-fuzzy controllers for integral plants to ensure robust stability. Information Sciences, 177(20) 4410–4429.
http://dx.doi.org/10.1016/j.ins.2007.05.005

Precup, R.-E., Preitl, S., Balas, M., & Balas, V. (2004). Fuzzy controllers for tire slip control in anti-lock braking systems. In Proceedings of IEEE International Conference on Fuzzy Systems (FUZZ-IEEE 2004), Budapest, Hungary, vol. 3, pp. 1317–1322.

Precup, R.-E., Preitl, S., Radac, M.-B., Petriu, E. M., Dragos, C.-A., & Tar, J. K. (2011d). Experiment-based teaching in advanced control engineering. IEEE Transactions on Education, 54(3) 345–355.
http://dx.doi.org/10.1109/TE.2010.2058575

Precup, R.-E., Tomescu, M. L., & Preitl, S. (2009). Fuzzy logic control system stability analysis based on Lyapunov's direct method. International Journal of Computers, Communications & Control, 4(4), 415–426.

Precup, R.-E., Tomescu, M. L., Radac, M.-B., Petriu, E. M., Preitl, S., & Dragos, C.-A. (2012b). Iterative performance improvement of fuzzy control systems for three tank systems. Expert Systems with Applications, 39(9) 8288–8299.
http://dx.doi.org/10.1016/j.eswa.2012.01.165

Preitl, S., & Precup, R.-E. (1996). On the algorithmic design of a class of control systems based on providing the symmetry of open-loop Bode plots. Scientific Bulletin of "Politehnica" University of Timisoara, Romania, Transactions on Automatic Control and Computer Science, 41(55:2) 47–55.

Preitl, S., & Precup, R.-E. (1997). Introducere in conducerea fuzzy a proceselor. Bucharest: Editura Tehnica.

Preitl, S., & Precup, R.-E. (1999). An extension of tuning relations after symmetrical optimum method for PI and PID controllers. Automatica, 35(10) 1731–1736.
http://dx.doi.org/10.1016/S0005-1098(99)00091-6

Preitl, S., Precup, R.-E., Fodor, J., & Bede, B. (2006). Iterative feedback tuning in fuzzy control systems. Theory and applications. Acta Polytechnica Hungarica, 3(3) 81–96.

Preitl, S., Preitl, Z., & Precup, R.-E. (2002). Low cost fuzzy controllers for classes of second-order systems. In Preprints of 15th IFAC World Congress, Barcelona, Spain, paper 416, 6 pp.

Shin, M. S., Ko, M. C., Ju, Y. W., Jung, Y. J., & Lee, B. J. (2013). Implementation of context-aware based robot control system for automatic postal logistics. Studies in Informatics and Control, 22(1) 71–80.

Sun, L. W., Van Meer, F., Bailly Y., & Yeung, C. K. (2007). Design and development of a Da Vinci surgical system simulator. In Proceedings of IEEE International Conference on Mechatronics and Automation (ICMA 2007), Harbin, China, pp. 1050–1055.

http://dx.doi.org/10.1109/ICMA.2007.4303693

Syed, A. A., Duan, X. G., Kong, X., Li, M., Wang, Y., & Huang, Q. (2012). 6-DOF Maxillofacial Surgical Robotic Manipulator Controlled By Haptic Device. In Proceedings of 9th International Conference on Ubiquitous Robots and Ambient Intelligence (URAI 2012), Daejeon, Korea, pp. 71–74. http://dx.doi.org/10.1109/URAI.2012.6462935

Škrjanc, I., & Blažič, S. (2005). Predictive functional control based on fuzzy model: design and stability study. Journal of Intelligent and Robotic Systems, 43(2–4) 283–299. http://dx.doi.org/10.1007/s10846-005-5138-9

Škrjanc, I., Blažič, S., Oblak, S., & Richalet, J. (2004). An approach to predictive control of multivariable time-delayed plant: Stability and design issues. ISA Transactions, 43(4) 585–595. http://dx.doi.org/10.1016/S0019-0578(07)60170-0

Takacs, A., Jordan, S., Precup, R.-E., Kovacs, L., Rudas, I. J., & Haidegger, T. (2014). Review of Tool–Tissue Interaction Models for Robotic Surgery Applications, In Proceedings of 12th IEEE International Symposium on Applied Machine Intelligence and Informatics (SAMI 2014), Herľany, Slovakia, pp. 339–344. http://dx.doi.org/10.1109/SAMI.2014.6822435

Tang, L., Zhao, Y., & Liu, J. (2014). An improved differential evolution algorithm for practical dynamic scheduling in steelmaking-continuous casting production. IEEE Transactions on Evolutionary Computation, 18(2) 209–225. http://dx.doi.org/10.1109/TEVC.2013.2250977

Tikk, D., Johanyák, Z. C., Kovács, S., & Wong, K. W. (2011). Fuzzy rule interpolation and extrapolation techniques: Criteria and evaluation guidelines. Journal of Advanced Computational Intelligence and Intelligent Informatics, 15(3) 254–263.

Tomescu, M. L., Preitl, S., Precup, R.-E., & Tar, J. K. (2007). Stability analysis method for fuzzy control systems dedicated controlling nonlinear processes. Acta Polytechnica Hungarica, 4(3) 127–141.

Vaščák, J. (2010). Approaches in adaptation of fuzzy cognitive maps for navigation purposes. In Proceedings of 8th International Symposium on Applied Machine Intelligence and Informatics (SAMI 2010), Herľany, Slovakia, pp. 31–36. http://dx.doi.org/10.1109/SAMI.2010.5423716

Vaščák, J., & Paľa, M. (2012). Adaptation of fuzzy cognitive maps for navigation purposes by migration algorithms. International Journal of Artificial Intelligence, 8(S12) 20–37.